

Removal of Phosphate from Aqueous Solutions by Chemical- and Thermal-Modified Bentonite Clay

Mehtap Tanyol · Vahap Yonten · Veysel Demir

Received: 7 May 2015 / Accepted: 7 July 2015 / Published online: 22 July 2015
© Springer International Publishing Switzerland 2015

Abstract The study investigated phosphate adsorption from aqueous solutions using chemical- and thermal-modified bentonite in batch system. The adsorbent was characterized by SEM, BET, and FTIR spectroscopy. Contact time, beginning phosphate concentration, pH of the solution, and the effects of the temperature on phosphate adsorption capacity were determined by a series of experimental studies. In a wide pH range (3–10), high phosphate removal yields were obtained (between 94.23 and 92.26 %), and with the increase in temperature (from 25 to 45 °C), phosphate removal increased. Langmuir and Freundlich isotherms were used to determine the sorption equilibrium, and the results demonstrated that equilibrium data displayed better adjustment to Langmuir isotherm than the Freundlich isotherm. Phosphate sorption capacity, calculated using Langmuir equation, is 20.37 mg g⁻¹ at 45 °C temperature and pH 3. Mass transfer and kinetic models were applied to empirical findings to determine the mechanism of adsorption and the potential steps that control the reaction rate. Both external mass transfer and intra-particle diffusion played

a significant role on the adsorption mechanism of phosphate, and adsorption kinetics followed the pseudo-second-order-type kinetic. Furthermore, thermodynamic parameters (ΔH° , ΔG° , ΔS°) which reveal that phosphate adsorption occur spontaneously and in endothermic nature were determined. The results of this study support that bentonite, which is found abundant in nature and modified as an inexpensive and effective adsorbent, could be used for phosphate removal from aqueous solutions.

Keywords Phosphate · Adsorption · Modified bentonite · Isotherm · Kinetic · Thermodynamic

1 Introduction

Phosphate is a macronutrient found in natural waters, with significance for various biological and chemical processes (Rodrigues and Silva, 2009). In aquatic environment, phosphorus compounds could be hydrolyzed to orthophosphate; however, only the phosphorus form could be used by bacteria, algae, and plants (Su et al., 2015). Phosphorus, in addition to human activities such as agricultural, industrial, and domestic use, could mix into the waters as a result of natural processes such as the disintegration of rocks (Das et al., 2006). In addition to being a nutrient, excess amounts of phosphate in water causes eutrophication, manifested in the existence of oxygen deficiency, decrease in aquatic species, and deterioration of water quality (Benyoucef and Amrani, 2011). Thus, excess phosphate in wastewaters should be

M. Tanyol (✉)
Department of Environmental Engineering, Tunceli
University, Tunceli, Turkey
e-mail: mtanyol@tunceli.edu.tr

V. Yonten
Department of Chemistry and Chemical Technology Process,
Vocational School, Tunceli University, Tunceli, Turkey

V. Demir
Department of Bioengineering, Tunceli University, Tunceli,
Turkey

removed before its discharge to aqueous environments like rivers or lakes. Traditional methods for phosphate removal include the following processes: sedimentation, coagulation/flocculation, ion exchange, reverse osmosis, complexation/sequestration, electrochemical treatment, biological treatment, and adsorption (Rodrigues and Silva, 2010). Furthermore, flotation is used for orthophosphate removal from wastewater (Karageorgiou et al., 2007). Among these methods, adsorption is considered as a rather effective removal method due to its high removal efficiency, economical usage in operations, and low waste production. Until today, several adsorbents including waste material and natural minerals such as orange waste (Biswas et al., 2008), rice hay (Cao et al., 2011), corncob (Wartelle and Marshall, 2006), banana stem (Anirudhan et al., 2006), goethite (Tribe and Barja, 2004), dolomite (Roques et al., 1991), alunite (Ozacar 2003), calcite (Liu et al. 2012), and bentonite clay (Dimirkou et al. 2002) were examined. Among these, bentonite is known as an inexpensive material, which is one of abundant clay minerals in earth and a great potential to be used as an adsorbent. Natural bentonite is an effective adsorbent for cations but displays lesser affinity against negative groups such as phosphate. Another disadvantage is being far from satisfactory adsorption performance including rate and capacity; thus, several studies spent efforts to ameliorate this situation (Huang et al., 2014; El-Sergany and Shanableh 2012).

Recently, some studies concentrated on the modification of clay minerals by using different procedures to increase the phosphate adsorption capacities of adsorbents such as cation addition (Li et al., 2009) or coating (Yuan et al., 2009), yet there were not any studies on phosphate removal with bentonite treated with acid and heat.

The objective of this study is to scrutinize phosphate removal from aqueous solutions using bentonite modified as an adsorbent. Thus, the effects of the temperature, the pH, and the beginning phosphate concentration and contact time on phosphate removal were examined. Equilibrium isotherm data were applied on Langmuir and Freundlich isotherm models, and isothermal coefficients were identified. Sorption mechanisms and potential reaction rate controlling steps on modified bentonite were investigated using external mass transfer and intraparticle diffusion models. Pseudo-first- and -second-order kinetic models were used to analyze adsorption kinetics. Furthermore, thermodynamic parameters were calculated using adsorption data.

2 Materials and Methods

2.1 Preparation of Modified Bentonite

Bentonite samples used in the study were obtained from Tokat region in Turkey. Chemical composition of the bentonite was analyzed by X-ray fluorescence spectrometry and was found as follows (in mass, %): SiO₂ 62.0, Al₂O₃ 17.5, Fe₂O₃ 3.5, CaO 3.5, Na₂O 2.7, K₂O 2.0, MgO 0.95, others (7.85). Crude bentonite was dried in oven at 105 °C for 1 day; 25 g of crude bentonite was added slowly to 100 mL 0.75 M nitric acid solution. The mixture was then stirred and was kept at boiling temperature for approximately 120 min using a hotplate stirrer with condenser. Acid-activated bentonite was filtered and washed with deionized water until the pH of the filtrate was equal to 5. Final adsorbent was prepared by keeping the specimens in ash furnace for 180 min at 700 °C. Chemical- and thermal-modified bentonite was then pulverized to rid of pellets formed during searing and preserved in a closed bottle for further use in the adsorption studies.

2.2 Chemicals

Stock solution of phosphate was prepared by dissolving the necessary amount of potassium dihydrogen phosphate (KH₂PO₄) (Merck) in 1 L distilled water. Test solutions were prepared by diluting the stock solution to desired concentrations. Concentration range for these solutions was between 25 and 150 mg L⁻¹. pH values for each solution were adjusted to the required value before contact with sorbent using diluted and concentrated HCl (Merck) and NaOH (Merck) solutions.

2.3 Adsorption Studies

Adsorption experiments were conducted in 250-mL Erlenmeyer flasks by adding 0.5 modified bentonite to 100 mL phosphate solution under the desired concentration, temperature, and pH and under 250 rpm agitating rate; 5-mL samples were taken from the solution in predetermined intervals during the stirring process to determine the phosphate concentration remaining in the medium. Before the analysis, the samples were filtered through a 0.45 membrane syringe filter and analyzed for remaining supernatant fluid phosphate amount. All experiments were repeated twice, and average values were used for future calculations.

2.4 Analysis

The non-adsorbed phosphate concentration in adsorption medium was determined using spectrophotometry with molybdovanadate methods (Hach DR-890). To determine the particle size distribution of modified bentonite samples, Mastersizer 3000 particle size analyzer was used. Surface morphologies of the samples were analyzed with Leo 1430 VP scanning electron microscopy. BET surface areas were determined from nitrogen adsorption isotherms using Micromeritics Gemini 2360 Surface Area Analyzer. The infrared spectrum of the samples was found by a Thermo Nicolet iS10 FT-IR Spectrometer.

2.5 Adsorption Yield and Adsorption Capacity

Adsorption data for the phosphate retention on modified bentonite were examined under various beginning concentrations, pH values, and temperatures. The results were given as adsorbed phosphate amount unit per modified bentonite gram at any given time (q) and equilibrium (q_{eq}) and non-adsorbed phosphate concentration left in the solution under any given time (C) and equilibrium (C_{eq}). Adsorption yield was calculated using the following formula:

$$\text{Ads. yield \%} = 100 \times \frac{(C_0 - C_{eq})}{C_{eq}} \quad (1)$$

Adsorption capacity was calculated as follows:

$$q = \frac{(C_0 - C)}{X} \quad (2)$$

2.6 Adsorption Equilibrium

To understand the mechanism of adsorption process, empirical data were applied to classical Langmuir (Langmuir, 1918) and Freundlich (Freundlich, 1906) models. Langmuir isotherm is basically used to explain the monolayer adsorption process. Langmuir equation is expressed with the following relationship:

$$q_{eq} = \frac{q_m b C_{eq}}{1 + b C_{eq}} \quad (3)$$

where q_{eq} is the adsorbed phosphate amount at the time of equilibrium (mg g^{-1}), C_{eq} is the equilibrium concentration of the phosphate in the solution (mg L^{-1}), q_m is

the maximum adsorption capacity (mg g^{-1}), and b is the adsorption equilibrium constant related to the adsorption energy (L mg^{-1}).

Freundlich model assumes that the adsorption occurs on heterogeneous surfaces. It is given as the Freundlich equation:

$$q_{eq} = K_f C_{eq}^{1/n} \quad (4)$$

where K_f is the relative adsorption capacity, and n is a constant dependent on the adsorption density.

2.7 Adsorption Kinetics

To determine the mechanisms that control adsorption, four kinetic models, namely, external mass transfer model, intra-particle mass transfer diffusion model, the pseudo-first-order and pseudo-second-order models, were implemented to fit the data (The kinetic equations used were followed from Dursun and Tepe (2011) and Dursun et al. (2013)). Based on the external mass transfer model (Findon et al., 1993; McKay 1983), the change in phosphate concentration in time is related to the liquid–solid external mass transfer coefficient k_L (cm min^{-1}):

$$\frac{d(C/C_0)}{dt} = -k_L S \quad (5)$$

where C is the dissolved substance concentration of phosphate in t time in liquid phase (mg L^{-1}), C_0 is the beginning phosphate concentration (mg L^{-1}), and S is the specific surface area for mass transfer.

$$S = \frac{6X}{d_p \rho_p} \quad (6)$$

where X is the sorbent concentration in the solution (g L^{-1}), d_p is the average particle diameter (cm), and ρ_p (g cm^{-3}) is the sorbent density.

The rate of intra-particle diffusion is a function of $t^{1/2}$ and could be given as the following equation (Weber and Morris, 1963):

$$q = f \left(\frac{Dt}{r_p^2} \right) = K t^{0.5} \quad (7)$$

where r_p is the particle radius, D is the intra-particle diffusion coefficient, and K is the intra-particle diffusion constant. K values could be determined by linearizing the $q = f(t^{0.5})$ curve (Choy et al. 2004).

The simple form of the pseudo-first order equation could be given using the Lagergreen equation (Lagergren, 1898):

$$\log(q_{\text{eq}} - q_t) = \log q_{\text{eq}} - \frac{k_1 t}{2.303} \quad (8)$$

where q is the adsorbed phosphate amount per gram adsorbent in any given time (mg g^{-1}), and k_1 is the rate constant for pseudo-first-order sorption (min^{-1}).

A pseudo-second-order equation based on the adsorption equilibrium capacity may be expressed in the following form (Ho and McKay, 1999):

$$\frac{t}{q} = \frac{1}{k_2 q_{\text{eq}}^2} + \frac{1}{q_{\text{eq}}} t \quad (9)$$

where k_2 is the velocity constant for pseudo-second-order sorption.

Standard error values normalized for the pseudo-first-order and pseudo-second-order equations were determined using Eq. (10) (Wu et al., 2009), where the indices of “exp” and “cal” denote empirical and calculated values, respectively, and N denotes the number of data.

$$\text{SD}(\%) = 100 \sqrt{\frac{\sum \left(\frac{(q_{t,\text{exp}} - q_{t,\text{cal}})}{q_{t,\text{exp}}} \right)^2}{N-1}} \quad (10)$$

2.8 Adsorption Thermodynamics

The three thermodynamic parameters, namely, Gibbs free energy (ΔG°), enthalpy (ΔH°), and entropy (ΔS°), were calculated to determine the nature of adsorption process and the thermodynamic compliance for the phosphate adsorption on modified bentonite. These parameters were calculated using the equations given below (Zhang et al., 2013):

$$\Delta G^\circ = -R T \ln K_1 \quad (11)$$

where R is the ideal gas constant ($8.314 \text{ Jmol}^{-1} \text{ K}^{-1}$), T is the absolute (Kelvin) temperature (K), and K_1 is the thermodynamic equilibrium constant.

$$\ln K_1 = \frac{\Delta S^\circ}{R} - \frac{\Delta H^\circ}{RT} \quad (12)$$

ΔH° and ΔS° values could be found by the slope and skew of the $\ln K_1$ curve against $1/T$.

3 Results and Discussion

3.1 Characterization of the Adsorbent

Particle size distribution for modified clay samples are displayed in Fig. 1. It was determined that 10 % of the modified bentonite particles were smaller than $8.13 \mu\text{m}$, 50 % were smaller than $31.3 \mu\text{m}$, and 90 % were smaller than $110 \mu\text{m}$. Thus, it could be argued that the particle size of 80 % of the sample was between 8.13 and $110 \mu\text{m}$.

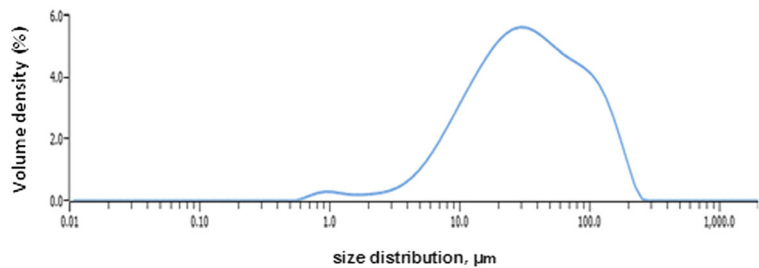
Crude bentonite and modified bentonite surface areas were determined with the BET surface area measurements as 8.844 and $15.518 \text{ m}^2/\text{g}$, respectively. The acid treatment and the following thermal treatment increased the surface area of the crude bentonite.

SEM images help understand the microscale surface morphology of the bentonite samples. As can be seen in Fig. 2, bentonite surface is relatively more smooth and flat than crude bentonite after the acid and thermal treatments. After adsorption, modified bentonite surfaces became swollen. This swelling could be the result of phosphate adsorption.

FT-IR spectra for bentonite samples are available in Fig. 3. In the IR diagrams, the basic stretch and each vibration of raw bentonite are given in Fig. 3. O–H stretching absorption bond and O–H stretching bonds (Al–OH, Si–OH, Al–Al–OH, Mg–Al–OH) that are inside the lattice were observed at 3699 and 3618 cm^{-1} , respectively. Bands and peaks at 1172 and 1080 cm^{-1} correspond to Si–O–Si; at 979 , 694 , and 524 cm^{-1} to Si–O–Al; 794 and 609 cm^{-1} to Si–O–Si and Si–O–Al. The stretching bonds of OH molecules in raw bentonite at 3699 and 3618 cm^{-1} did not appear in modified bentonite when considered to the comparison of raw and modified bentonite. The power adsorbent of clays to absorb the anions has been thought about Fe and Al complex (Dimirkou et al. 2002; Yonten and Kubilay 2011; Ye et al. 2006).

Then, the anion adsorption capacities were decreased or completely destroyed while these metals disappeared from the medium. It is thought to be OH[−] ions and anions replaced in anion adsorption on raw clay minerals. In this work, the phosphate ions replacing the OH[−] ions were in bentonite structure. Because of calcinations, O–H stretching bonds at 3699 and 3618 cm^{-1} disappeared, and at 3441 cm^{-1} , the existence of O–H stretching bonds in modified bentonite shows that there are P–OH stretching bonds. In light of these, it could be an evidence for bentonite adsorbing the phosphate.

Fig. 1 Particle size distribution of modified bentonite particles



3.2 Effects of the Contact Time

Figure 4 shows the change in phosphate adsorption capacity with time on modified bentonite at 25, 35, and 45 °C. Adsorption studies were continued for 180 min, and it was found that adsorption capacity increased with

the increasing contact time and temperature, and a large portion of the phosphate was removed during the first 60 min of adsorption. Under all temperatures, the equilibrium was attained within 90 min after rapid adsorption. An adsorption process taking a short time provides advantages for large-scale applications.

3.3 Effects of Initial Solution pH

As is known, phosphate anions could be found in different ionic forms depending on the pH of the solution, namely, as H_2PO_4^- , HPO_4^{2-} , and PO_4^{3-} in water. In the pH range 7.2 and 10.0, the dominant phosphate type is HPO_4^{2-} , while in the pH range 3.0–7.2, the main monovalent ion is H_2PO_4^- (Tang et al. 2014). It is well known that certain anions (i.e., phosphate, nitrate, and arsenate) are adsorbed via electrostatic attraction and ligand exchange. In the pH range 3.0–6.0, adsorption occurs through the ion exchange mechanism of phosphate hydrolysis products ($\text{H}_2\text{PO}_4^{1-}$, HPO_4^{2-}). Furthermore, due to their competition with OH ions, higher pH level could reduce PO_4^{3-} bonding capacity on adsorbent surface (Oguz et al., 2003).

Tests were conducted with different starting pH values changing between 3 and 10 to determine the effect of starting pH level on phosphate removal in the aqueous system. Figure 5 demonstrates the change in phosphate concentration retained in equilibrium based on the starting pH. Phosphate removal with modified bentonite reduced with the increasing pH, but the dependency of removal on pH was not high. The highest adsorption capacity was found as 14.18 mg g^{-1} at pH 3, while at pH 10, it was reduced to 13.20 mg g^{-1} , and phosphate removals in these pH levels were found to be 94.53 and 92.26 %, respectively. Obtaining high yield in all pH levels and especially at neutral pH (93.33 % removal) is significant in achieving the standards for discharge to the receiving environment of the treated wastewaters.

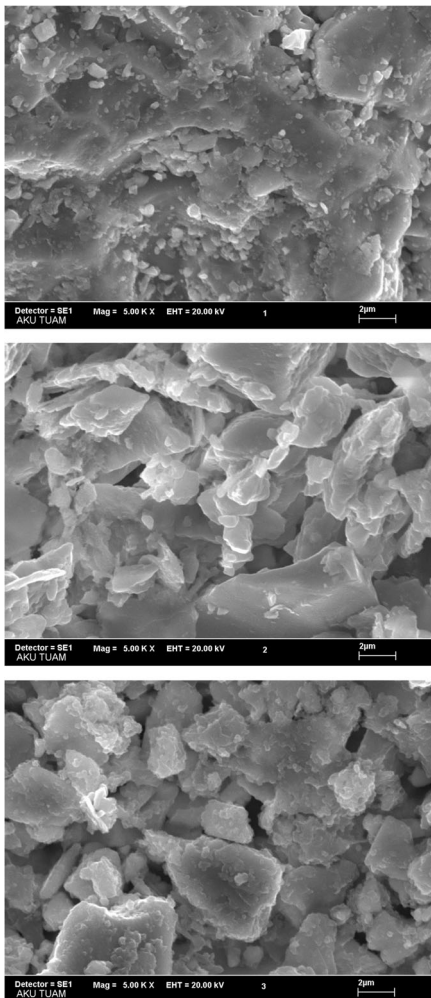
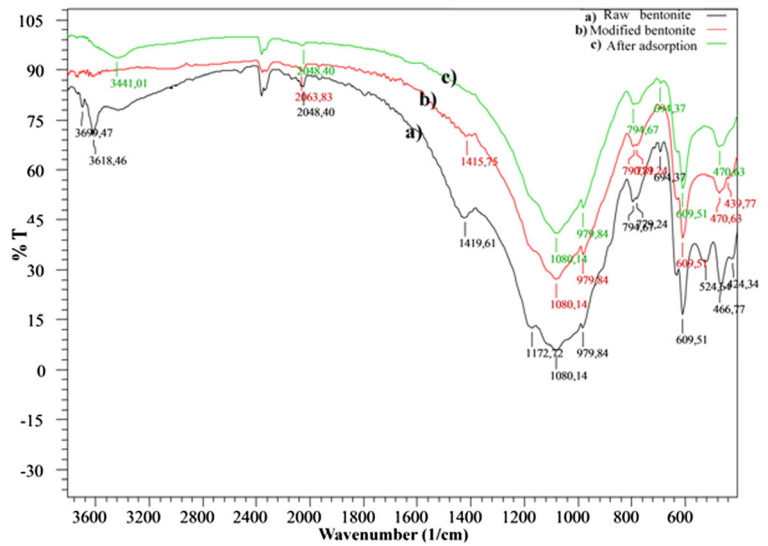


Fig. 2 SEM images of the bentonite. 1 crude bentonite, 2 modified bentonite, 3 bentonite after adsorption

Fig. 3 Bentonite IR spectra



3.4 Effects of Initial Phosphate Concentration on the Temperature Dependence of Adsorption

The effects of the temperature on phosphate removal with modified bentonite were scrutinized in different initial phosphate concentrations and within the temperature range of 25–45 °C. Table 1 displays the results for 25–150 mg L⁻¹ initial phosphate concentrations. Phosphate removal increased with the increasing temperature and reached to 21.12 mg g⁻¹ at 45 °C. The increase in adsorption with the increase in temperature could be related to the increase in active surface areas on adsorbent suitable for adsorption and also to the increase in porosity and total porous volume of the adsorbent. The increase in adsorption could also be related to the decrease in the thickness of the border layer encompassing the sorbent

with heat and thus the decrease in the mass transfer resistance of the phosphate in the border layer. At the same time, this may be the result of the increase in mobility of phosphate with increasing kinetic energy and the increase in internal diffusion rate of the phosphate with increasing temperature. This indicates that the phosphate adsorption on modified bentonite is endothermic, and the process could both contain physical and chemical adsorption. Table 1 also demonstrates the effects of the initial phosphate concentration on modified bentonite. As a rule, the increase in beginning phosphate concentration, since the original phosphate concentration provides a driving force to overcome the mass transfer resistance between the adsorbent and the adsorption environment, results in an increase in adsorption capacity. Thus, in all temperatures at which the study was conducted, higher adsorption capacities were obtained in higher initial

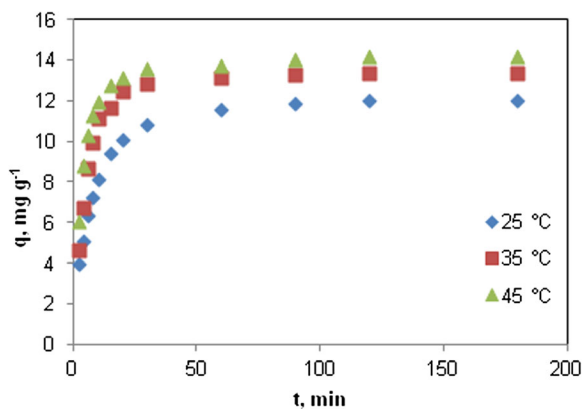


Fig. 4 Adsorption curves for phosphate removal ($C_o=75$ mg L⁻¹, pH 3.0, $X=0.5$ g 100 m L⁻¹, agitation rate = 250 rpm)

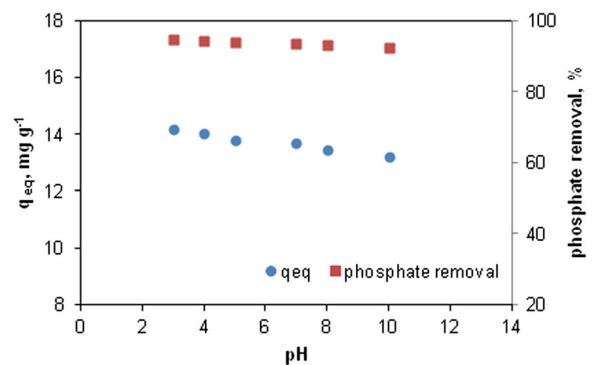


Fig. 5 The effects of pH on phosphate adsorption ($C_o=75$ mg L⁻¹, $T=45$ °C, $X=0.5$ g 100 m L⁻¹, agitation rate = 250 rpm)

Table 1 Equilibrium adsorption capacities and adsorption yield obtained with different initial phosphate concentrations and temperatures

C_0 (mg L ⁻¹)	25 °C		35 °C		45 °C	
	q_{eq} (mg g ⁻¹)	Adsorption (%)	q_{eq} (mg g ⁻¹)	Adsorption (%)	q_{eq} (mg g ⁻¹)	Adsorption (%)
25	4.56	91.20	4.78	95.6	4.86	97.20
50	8.76	87.60	9.12	91.2	9.52	95.20
75	11.60	77.33	13.36	89.07	14.18	94.53
100	12.82	64.10	16.22	81.02	17.04	85.20
150	14.88	49.60	17.28	57.60	21.12	70.40

concentrations. Table 1 displays furthermore the adsorption yields determined in different initial phosphate concentrations and phosphate amounts adsorbed in the equilibrium. Generally, the increase of phosphate concentration resulted in a decrease in adsorption yield, and the maximum adsorption yield was determined as 97.2 % at 45 °C temperature and in 25 mg/L initial concentration. With lower initial concentrations, the amount of phosphate is lower as compared to the existing adsorption areas, and higher adsorption yields are obtained. In higher concentrations, saturation of adsorbent bonding locations causes a decrease in the adsorption. This was the cause of the decrease observed in adsorption yields.

When the modified bentonite used in the study (21.12 mg g⁻¹ for 150 mg/L phosphate concentration at 45 °C and pH 3, BET surface area 15.518 m² g⁻¹) is compared with other results in the literature, it could be concluded that modified bentonite was effective for this purpose. Huang et al. (2008) used acid- and thermal-treated red mud, an alumina refinery waste, for phosphate removal. BET surface areas of crude red mud and acid- and acid-thermal-treated adsorbents were found as 27.71, 28.48, and 33.78 m² g⁻¹, respectively. The highest adsorption capacity was obtained from HCl-treated red

mud at pH 5.5 and 40 °C as 0.58 mg g⁻¹. Kuroki et al. (2014) removed phosphate from aqueous solutions using bentonite procured from Northern Brazil and treated with lanthanum (NT-25La). They have reported that the adsorption process has reached the equilibrium in 60 min, and the maximum phosphate sorption capacity was 14.0 mg g⁻¹ at 333 K (BET surface area 134 m² g⁻¹). Zamparas et al. (2012) studied phosphate removal from natural waters using modified inorganic bentonite (Zenith/Fe) prepared by placing Fe ions in natural bentonite interface. Phosphate removal of the modified bentonite was found to be 350 % more than that of the non-modified bentonite (11.15 and 4.12 mg g⁻¹, respectively). For optimum phosphate removal, a pH range of 6–7 and 35 °C temperature were established. Yan et al. (2010) prepared three modified inorganic bentonites—hydroxy–aluminum-pillared bentonite (Al-Bent), hydroxy–iron-pillared bentonite (Fe-Bent), and mixed hydroxy-iron–aluminum-pillared bentonite (Fe–Al-Bent)—and compared the phosphorus removal capacities of these bentonites. Phosphate adsorption capacities were as follows, respectively: 12.7, 11.2, and 10.5 mg g⁻¹; Al-Bent > Fe-Bent > Fe–Al-Bent. Phosphorus adsorption capacities reached the maximum

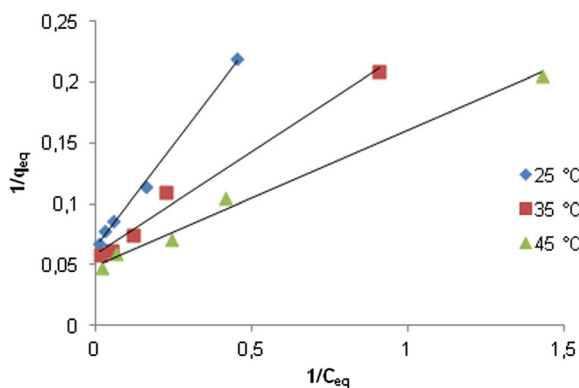
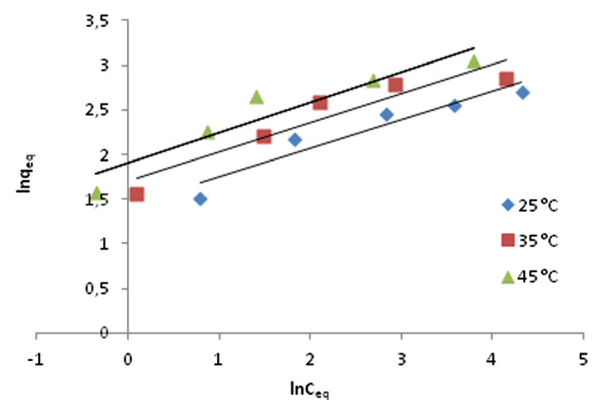
**Fig. 6** Linearized Langmuir adsorption isotherm of phosphate**Fig. 7** Linearized Freundlich adsorption isotherm of phosphate

Table 2 Isotherm coefficients for phosphate adsorbed on modified bentonite

T, °C	Langmuir model			Freundlich model		
	q_{max}	b	R^2	K_f	N	R^2
25	15.45	0.1919	0.9969	3.88	3.14	0.9969
35	17.33	0.3404	0.9855	4.61	3.06	0.9049
45	20.37	0.4423	0.9908	5.17	2.93	0.9105

at pH value of 3 for three inorganic pillared bentonites. Their BET surface areas were reported as 200, 143, and 94.9 m² g⁻¹, respectively. Xie et al. (2015) determined the phosphate removal capacities for activated aluminum oxide (AAO) and lanthanum oxide (LO) as 20.88 and 46.95 mg g⁻¹, respectively. Phosphate removal with AAO was effective under acidic conditions (pH<5.0), while phosphate removal with LO was not effected highly under pH 10.5. Specific surface areas for AAO and LO were determined as 298.3 and 12.0 m² g⁻¹, respectively. Zeng et al. (2004) conducted their studies using iron oxide tailings and found the optimum pH as 3.2 and maximum removal capacity as 8.6 mg g⁻¹.

3.5 Determination of Equilibrium Parameters

The equilibrium parameters provide basic requirements for the design of adsorption systems such as the relationship between the substance adsorbed and the adsorbent and information on the capacity of the adsorbent. In this study, the most frequently used isotherms in modeling the adsorption data, namely, the Langmuir and Freundlich equations, were utilized. In the study, while the adsorbent concentration was kept constant (0.5 g 100 mL⁻¹) for 25, 35, and 45 °C, initial phosphate

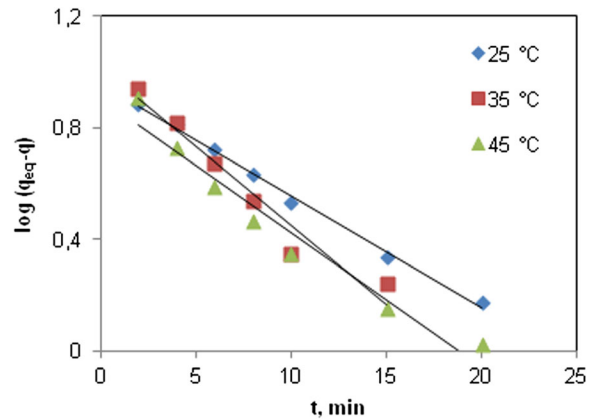


Fig. 8 Pseudo-first-order adsorption kinetics of phosphate at different temperatures

concentrations were altered between 25 and 150 mg/L. Figures 6 and 7 demonstrate the linearized isotherm curves for Langmuir and Freundlich equations, respectively. Table 2 shows the values of adsorption model coefficients showing surface characteristics, the adsorption mechanism and capacity or affinity of the sorbent. K_f , one of the Freundlich coefficients, is used as the relative measurement of adsorption capacity. K_f values increased with increasing temperatures and were determined highest as 5.16 at 45 °C. Another Freundlich coefficient, the n value, is an empirical parameter that changes with the degree of heterogeneity that shows the non-linear step between phosphate retention capacity of the adsorbent and non-adsorbed phosphate concentration. At all temperatures, calculated n values are over 1. The fact that n values were over 1 demonstrated that all temperatures studied were effective for the process of phosphate adsorption. As the temperature rose from 25 to 45 °C, q_{max} and b values calculated with the Langmuir equation rose from 15.45 to 20.37 and from 0.19 to 0.44, respectively. q_{max} , denominating the

Table 3 Exchange with initial phosphate concentration and temperature on the external mass transfer coefficients (k_L) and intraparticle diffusion rate constants (K)

C_o (mg L ⁻¹)	25 °C		35 °C		45 °C	
	k_L (cm min ⁻¹)	K (mg g ⁻¹ min ^{-0.5})	k_L (cm min ⁻¹)	K (mg g ⁻¹ min ^{-0.5})	k_L (cm min ⁻¹)	K (mg g ⁻¹ min ^{-0.5})
25	0.016581	0.032	0.018491	0.036	0.036635	0.041
50	0.010461	0.094	0.014151	0.148	0.016191	0.267
75	0.007379	0.153	0.008334	0.242	0.009914	0.514
100	0.005447	0.164	0.005495	0.271	0.007451	0.055
150	0.002734	0.19	0.003781	0.298	0.006685	0.588

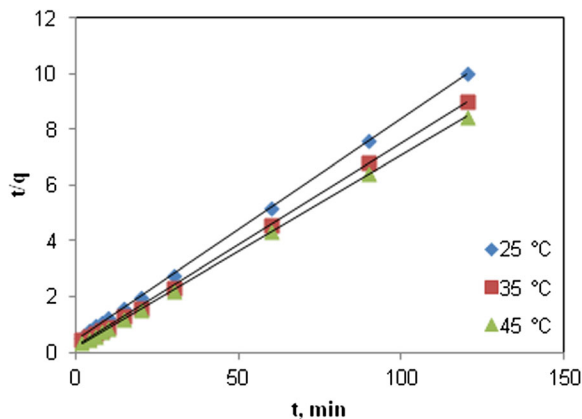


Fig. 9 Pseudo-second-order adsorption kinetics of phosphate at different temperatures

maximum capacity, indicates the total capacity of adsorbent for phosphate, or inlayer saturation in equilibrium. The other Langmuir constant, *b*, shows the interest of the adsorbent for the phosphate bond. The highest *b* value found at 45 °C shows that at that temperature phosphate bonds with the adsorbent strongly. Table 2 demonstrates that adsorption values correlated with the Langmuir model better fit than the other model when the correlation coefficients of the two isotherm models were compared.

3.6 Kinetic Parameters of Adsorption

Batch adsorption studies were conducted to define the potential steps that control the reaction rate for the design and evaluation of the adsorbent. External film mass transfer, intraparticle diffusion and pseudo-first- and -second-order kinetic models were used to test the dynamics of the sorption process, and the experiments were conducted to calculate the coefficients of these models. For the system where external mass transfer was studied, the solute is characterized by the beginning rate of the diffusion. In *C/C₀* curves against the *t* found at 25, 35, and 45 °C (undisclosed data) and in all initial phosphate

concentrations and in all internal diffusion conditions, the findings demonstrated that the phosphate concentration decreased rapidly along the initial adsorption before internal diffusion controls adsorption kinetics in all conditions. External mass transfer coefficients were determined from the slopes as *t*→0 and displayed in Table 3. Findings showed that as the initial phosphate concentration increased, external mass transfer coefficients and external mass transfer decreased. Furthermore, along with the increasing temperature, external mass transfer coefficient values increased. This could be the result of the increase in external mass transfer rate as a result of the increase in the mobility of phosphate molecules together with the increase in temperature due to the rise in the kinetic energy of the phosphate molecules. Although this effect is only significant in the initial period of the adsorption, it is obvious that external mass transfer could not be disregarded.

The curves of *q* against *t*^{0.5} plotted for all initial phosphate concentrations and at 25, 35, and 45 °C (undisclosed data) revealed that all the plots have the same general feature representing multilinearity, indicating that a few steps took place. The first part, a sharply increasing section, found in the initial period related to the initial phosphate concentration and temperature is attributed to the diffusion of the substance adsorbed on the external surface of the adsorbent from the solution or to the border layer diffusion of the solved molecules. The second linear part showing the intra-particle diffusion, a rate-limiting step, demonstrates the gradual layer adsorption stage. The third part shows the final equilibrium displaying the slowing down internal diffusion due to the low phosphate concentration left in the solution. For each concentration and temperature, linear curves of the second part did not pass through the origin. This indicates that the border layer control had some steps, and it also shows that intra-particle diffusion was not the step solely controlling the rate. *K* values for the curves calculated for these linear parts are displayed in Table 3. The

Table 4 The effects of the temperature on pseudo-first-order and -second-order reaction rate constants

<i>T</i> (°C)	<i>q_{eq}</i> (mg g ⁻¹)	Pseudo-first-order kinetic model			Pseudo-second-order kinetic model		
		<i>k₁</i> (min ⁻¹)	<i>q_{eq,cal}</i> (mg g ⁻¹)	<i>R</i> ²	<i>k₂</i> (min ⁻¹)	<i>q_{eq,cal}</i> (mg g ⁻¹)	<i>R</i> ²
25	11.60	0.09281	9.12	0.9961	0.01527	12.54	0.9998
35	13.36	0.11077	10.46	0.9473	0.02405	13.73	0.9997
45	14.18	0.13104	8.08	0.9537	0.03024	14.43	0.9999

Table 5 Change of thermodynamic parameters with temperature for phosphate adsorption

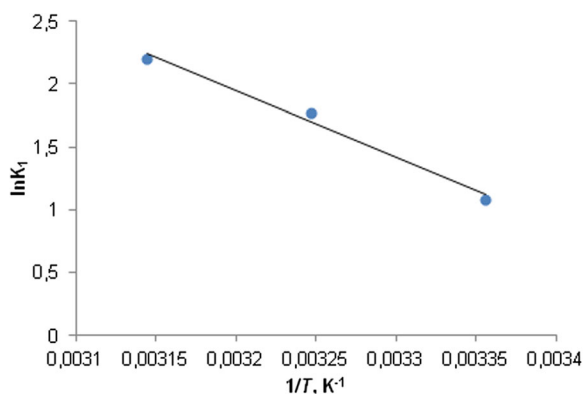
T °C	b L mg ⁻¹	ΔH° kJ mol ⁻¹	ΔG° kJ mol ⁻¹	ΔS° kJ mol ⁻¹ K ⁻¹
25	0.1919		-2.69	
35	0.3404	43.85	-4.54	0.16
45	0.4423		-5.81	

table shows that K values increased with the increasing initial phosphate concentrations and temperature.

Linearized curves for pseudo-first-order and pseudo-second-order equations are displayed in Figs. 8 and 9, respectively. k_1 , k_2 , q_{den} and correlation coefficients of these models were compared in Table 4. The table demonstrates that albeit the correlation coefficients for both models were high, they were higher for the second-order kinetic model. Concurrently, theoretical q_{den} values and empirical q_{den} values corresponded to the second-order kinetics better. To compare the quantitative applicability of each model, normalized standard deviation values were calculated. Normalized standard deviation value found for pseudo-first-order (48.65) was higher than the normalized standard deviation value found for pseudo-second-order (4.58). This demonstrates that pseudo-second-order kinetics could be defined as a rate-controlling step together with external mass transfer and internal diffusion.

3.7 Thermodynamic Study

Gibbs free energy change for the adsorption process was calculated using the equilibrium constants found by the Langmuir model (Table 5 and Fig. 10). The table

**Fig. 10** $\ln K_1$ vs. $1/T$ plot

demonstrates that all Gibbs free energy values are negative. Negative values of ΔG° show the suitability of the process and spontaneous nature of adsorption. Standard enthalpy change for adsorption was found to be 43.85 kJ/mol. Positive value of ΔH° supports the endothermic nature of adsorption. Entropy change of adsorption was determined as 0.16 kJ/mol K. Positive value of ΔS° shows the increasing randomness in solid-solution interphase during adsorption.

4 Conclusions

Acid- and thermal-modified bentonite was scrutinized for phosphate removal from aqueous solutions. The chemical and thermal process conducted increased the surface area of the adsorbent. Adsorption process was not affected by pH changes that much; however, with the increase in temperature, phosphate adsorption increased. Adsorption equilibrium was attained in 90 min. The highest adsorption capacity was found with 150 mg L⁻¹ initial phosphate concentration, at 45 °C and pH 3, as 21.12 mg g⁻¹. Adsorption equilibrium findings fit with the Langmuir isotherm model better when compared to the Freundlich isotherm model. The sorption process was found to be controlled by both external mass transfer and intraparticle diffusion with external mass transfer at the earlier stages followed by intraparticle diffusion at the later stages. Adsorption kinetics fitted the best with the pseudo-second-order model. Thermodynamically negative ΔG° , positive ΔH° , and positive ΔS° demonstrated the high affinity, spontaneous, and endothermic adsorption process between the adsorbent and the adsorbed. The adsorbent used in this study demonstrated a relatively good phosphate adsorption capacity and removal yield when compared to studies conducted with bentonite modified with different methods or with other adsorbents.

Acknowledgments This work was supported by Tunceli University Scientific Research Projects Unit (Project No. MFTUB 013–10).

References

- Anirudhan, T. S., Noeline, B. F., & Manohar, D. M. (2006). Phosphate removal from wastewaters using a weak anion exchanger prepared from a lignocellulosic residue. *Environmental Science & Technology*, 40, 2740–2745.

- Benyoucef, S., & Amrani, M. (2011). Adsorption of phosphate ions onto low cost aleppo pine adsorbent. *Desalination*, 275, 231–236.
- Biswas, B. K., Inoue, K., Ghimire, K. N., Harada, H., Ohto, K., & Kawakita, H. (2008). Removal and recovery of phosphorus from water by means of adsorption onto orange waste gel loaded with zirconium. *Bioresource Technology*, 99, 8685–8690.
- Cao, W., Danga, Z., Zhou, X. Q., Yi, X. Y., Wu, P. X., Zhua, N. W., & Lu, G. N. (2011). Removal of sulphate from aqueous solution using modified rice straw: preparation, characterization and adsorption performance. *Carbohydrate Polymers*, 85, 571–577.
- Choy, K. K. H., Porter, J. F., & McKay, G. (2004). Intraparticle diffusion in single and multicomponent acid dye adsorption from wastewater onto carbon. *Chemical Engineering Journal*, 103, 133–145.
- Das, J., Patra, B. S., Baliarsingh, N., & Parida, K. M. (2006). Adsorption of phosphate by layered double hydroxides in aqueous solutions. *Applied Clay Science*, 32, 252–260.
- Dimirkou, A., Ioannou, A., & Doula, M. (2002). Preparation, characterization and sorption properties for phosphates of hematite, bentonite and bentonite–hematite systems. *Advances in Colloid and Interface Science*, 97, 37–60.
- Dursun, A. Y., & Tepe, O. (2011). Removal of Chemazol Reactive Red 195 from aqueous solution by dehydrated beet pulp carbon. *Journal of Hazardous Material*, 194, 303–311.
- Dursun, A. Y., Tepe, O., & Dursun, G. (2013). Use of carbonised beet pulp carbon for removal of Remazol Turquoise Blue-G 133 from aqueous solution. *Environmental Science and Pollution Research*, 20(1), 431–442.
- El-Sergany, M., & Shanableh, A. (2012). Phosphorus removal using Al-modified bentonite clay-effect of particle size. *Asia Pacific Conference on Environmental Science and Technology Advances in Biomedical Engineering*, 6, 323–329.
- Findon, A., McKay, G., & Blair, H. S. (1993). Transport studies for the sorption of copper ions by chitosan. *Journal of Environmental Science and Health, Part A*, 28, 173–185.
- Freundlich, H. M. F. (1906). Over the adsorption in solution. *The Journal of Physical Chemistry*, 57A, 385–470.
- Ho, Y. S., & McKay, G. (1999). Pseudo-second order model for sorption processes. *Process Biochemistry*, 34, 451–465.
- Huang, W., Wang, S., Zhu, Z., Li, L., Yao, X., Rudolph, V., & Haghseresht, F. (2008). Phosphate removal from wastewater using red mud. *Journal of Hazardous Material*, 158, 35–42.
- Huang, W. Y., Li, D., Liu, Z. Q., Tao, Q., Zhu, Y., Yang, J., & Zhang, Y. M. (2014). Kinetics, isotherm, thermodynamic, and adsorption mechanism studies of La(OH)₃-modified exfoliated vermiculites as highly efficient phosphate adsorbents. *Chemical Engineering Journal*, 236, 191–201.
- Karageorgiou, K., Paschalis, M., & Anastassakis, G. N. (2007). Removal of phosphate species from solution by adsorption onto calcite used as natural adsorbent. *Journal of Hazardous Material*, A139, 447–452.
- Kuroki, V., Bosco, G. E., Fadini, P. S., Mozeto, A. A., Cestari, A. R., & Carvalho, W. A. (2014). Use of a La(III)-modified bentonite for effective phosphate removal from aqueous media. *Journal of Hazardous Material*, 274, 124–131.
- Lagergren, S. (1898). About the theory of so-called adsorption of soluble substances. *Kungliga Svenska Vetenskapsakademiens Handlingar*, 24, 1–39.
- Langmuir, I. (1918). The adsorption of gases on plane surfaces of glass, mica and platinum. *Journal of the American Chemical Society*, 40(9), 1361–1403.
- Li, H., Ru, J., Yin, W., Liu, X., Wang, J., & Zhang, W. (2009). Removal of phosphate from polluted water by lanthanum doped vesuvianite. *Journal of Hazardous Material*, 168, 326–330.
- Liu, Q., Guo, L., Zhou, Y., Dai, Y., Feng, L., Zhou, J., Zhao, J., Liu, J., & Qian, G. (2012). Phosphate adsorption on biogenic calcium carbonate minerals: effect of a crystalline phase. *Desalination and Water Treatment*, 47(1–3), 78–85.
- McKay, G. (1983). The adsorption of dyestuffs from aqueous solution using activated carbon: analytical solution for batch adsorption based on external mass transfer and pore diffusion. *Chemical Engineering Journal*, 27, 187–196.
- Oguz, E., Gurses, A., & Yalcin, M. (2003). Removal of phosphate from waste water by adsorption. *Water Air & Soil Pollution*, 148, 279–287.
- Ozacar, M. (2003). Adsorption of phosphate from aqueous solution onto alunite. *Chemosphere*, 5, 321–327.
- Rodrigues, L. A., & Silva, M. L. C. P. (2009). An investigation of phosphate adsorption from aqueous solution onto hydrous niobium oxide prepared by co-precipitation method. *Colloids and Surfaces A: Physicochemical and Engineering Aspects*, 334, 191–196.
- Rodrigues, L. A., & Silva, M. L. C. P. (2010). Thermodynamic and kinetic investigations of phosphate adsorption onto hydrous niobium oxide prepared by homogeneous solution method. *Desalination*, 263, 29–35.
- Roques, H., Nugroho-Jeudy, L., & Lebugle, A. (1991). Phosphorus removal from wastewater by half-burned dolomite. *Water Resource*, 25, 959–965.
- Su, Y., Yang, W., Sun, W., Li, Q., & Shang, J. K. (2015). Synthesis of mesoporous cerium–zirconium binary oxide nanoadsorbents by a solvothermal process and their effective adsorption of phosphate from water. *Chemical Engineering Journal*, 268, 270–279.
- Tang, J., Chen, J., Huang, W., Li, D., Zhu, Y., Tong, Y., & Zhang, Y. (2014). Porous Pr(OH)₃ nanowires as novel high-performance adsorbents for phosphate removal. *Chemical Engineering Journal*, 252, 202–209.
- Tribe, L., & Barja, B. C. (2004). Adsorption of phosphate on goethite. An undergraduate research laboratory project. *Journal of Chemical Education*, 81(11), 1624–1627.
- Wartelle, L. H., & Marshall, W. E. (2006). Quaternized agricultural by-products as anion exchange resins. *Journal of Environmental Management*, 78, 157–162.
- Weber, W. J., & Morris, J. C. (1963). Kinetics of adsorption on carbon from solution. *Journal of the Sanitary Engineering Division - American Society of Civil Engineers*, 89, 31–39.
- Wu, F. C., Tseng, R. L., & Juang, R. S. (2009). Initial behavior of intraparticle diffusion model used in the description of adsorption kinetics. *Chemical Engineering Journal*, 153, 1–8.
- Xie, J., Lin, Y., Li, C., & Kong, D. H. (2015). Removal and recovery of phosphate from water by activated aluminum oxide and lanthanum oxide. *Powder Technology*, 26, 351–357.
- Yan, L., Xu, Y., Yu, H., Xin, X., Wei, Q., & Bin, D. (2010). Adsorption of phosphate from aqueous solution by

- hydroxy–aluminum, hydroxy–iron and hydroxy–iron–aluminum pillared bentonites. *Journal of Hazardous Material*, 179, 244–250.
- Ye, H., Chen, F., Sheng, Y., Sheng, G., & Fu, J. (2006). Adsorption of phosphate from aqueous solution onto modified palygorskites. *Separation and Purification Technology*, 50, 283–290.
- Yonten, V., & Kubilay, S. (2011). The adsorption of the 2,2-dichlorovinylphosphate on raw and modified bentonites. *Journal of Animal and Veterinary Advances.*, 10(22), 2975–2979.
- Yuan, X. Z., Pan, G., Chen, H., & Tian, B. H. (2009). Phosphorus fixation in lake sediments using LaCl_3 -modified clays. *Ecological Engineering*, 35, 1599–1602.
- Zamparas, M., Areti, G., Stathi, P., Deligiannakis, Y., & Zacharias, I. (2012). Removal of phosphate from natural waters using innovative modified bentonites. *Applied Clay Science*, 62–63, 101–106.
- Zeng, L., Li, X., & Liu, J. (2004). Adsorptive removal of phosphate from aqueous solutions using iron oxide tailings. *Water Research*, 38, 1318–1326.
- Zhang, J., Cai, D., Zhang, G., Cai, C., Zhang, C., Qiu, G., Zheng, K., & Wu, Z. (2013). Adsorption of methylene blue from aqueous solution onto multiporous palygorskite modified by ion beam bombardment: effect of contact time, temperature, pH and ionic strength. *Applied Clay Science*, 83–84, 137–143.